Electronic Supplementary Material (ESI) for Chemical Communications

Hybrid porous material from a pillar[5]arene and a poly(ionic liquid): selective adsorption of *n*-alkylene diols

Zibin Zhang,[a] Qiang Zhao,[b] Jiayin Yuan,*[b] Markus Antonietti,[b] and Feihe Huang*[a]

[a] *Department of Chemistry, Zhejiang University, Hangzhou 310027, P. R. China*

Email address: fhuang@zju.edu.cn.

[b] *Department of Colloid Chemistry, Max Planck Institute of Colloids and Interfaces, D-14424 Potsdam, Germany,*

Email address: jiayin.yuan@mpikg.mpg.de

Electronic Supplementary Information

1. Materials and methods

1,4-Dimethoxybenzene, boron trifluoride ethyl ether complex, ethyl bromoacetate, borontribromide, and lithium bis(trifluoromethanesulfonyl)imide were reagent grade and used as received. Solvents were either employed as purchased or dried according to procedures described in the literature. The preparation of poly(3-cyanomethyl-1-vinylimidazolium bis(trifuoromethanesulfonyl)imide) **2** (PCMVImTf$_2$N, 1.15 × 10^5 g/mol, PDI: 2.95) was reported before.[S1] ^{1}H NMR spectra were collected on a Bruker DPX-400 spectrometer at room temperature. Nitrogen (N_2) sorption experiments were performed with a Quantachrome Autosorb-1 or Quadrasorb at liquid nitrogen temperature, and data analysis was performed by Quantachrome software. The surface area and pore volume were calculated using the Brunaer–Emmett-Teller (BET) equation and the Barrett-Joyner-Halenda (BJH) method, respectively. Samples for BET measurements were degassed at 80 ℃ for 20 h before measurements. X-ray diffraction experiments were done with a Bruker D8 diffractometer using Cu Kα radiation (λ = 0.154 nm) and a scintillation counter. FT-IR spectra were performed on a BioRad 6000 FT-IR spectrometer; samples were measured in the solid state using a Single Reflection Diamond ATR. Scanning electron microscopy (SEM) was performed on a GEMINI LEO 1550 microscope at 3 kV, and samples were coated with gold before examination.

*2. Syntheses of **1** and **5***

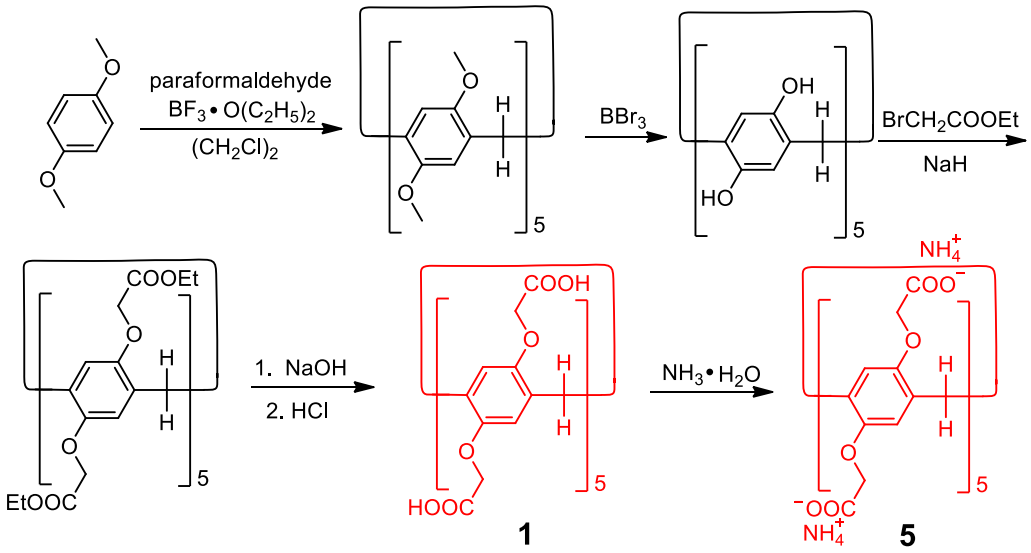

Scheme S1. Syntheses of **1** and **5**.[S2]

The fully carboxylic acid-substituted pillar[5]arene **1** and model compound **5** were prepared according to the literature methods.[S2] The proton NMR spectrum of **1** is shown in Fig. S1. The proton NMR spectrum of **5** is shown in Fig. S2.

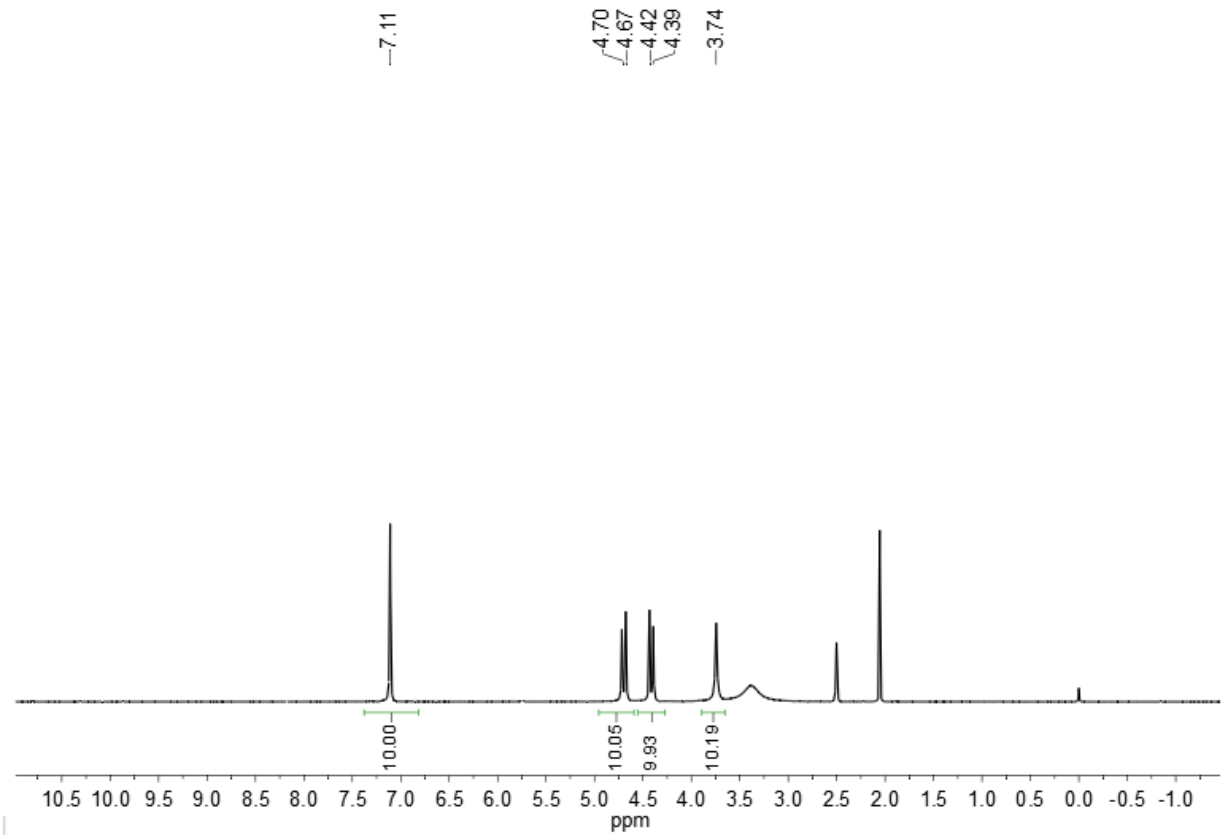

Fig. S1. ^{1}H NMR spectrum (400 MHz, DMSO-d_6, 20 °C) of **1**.

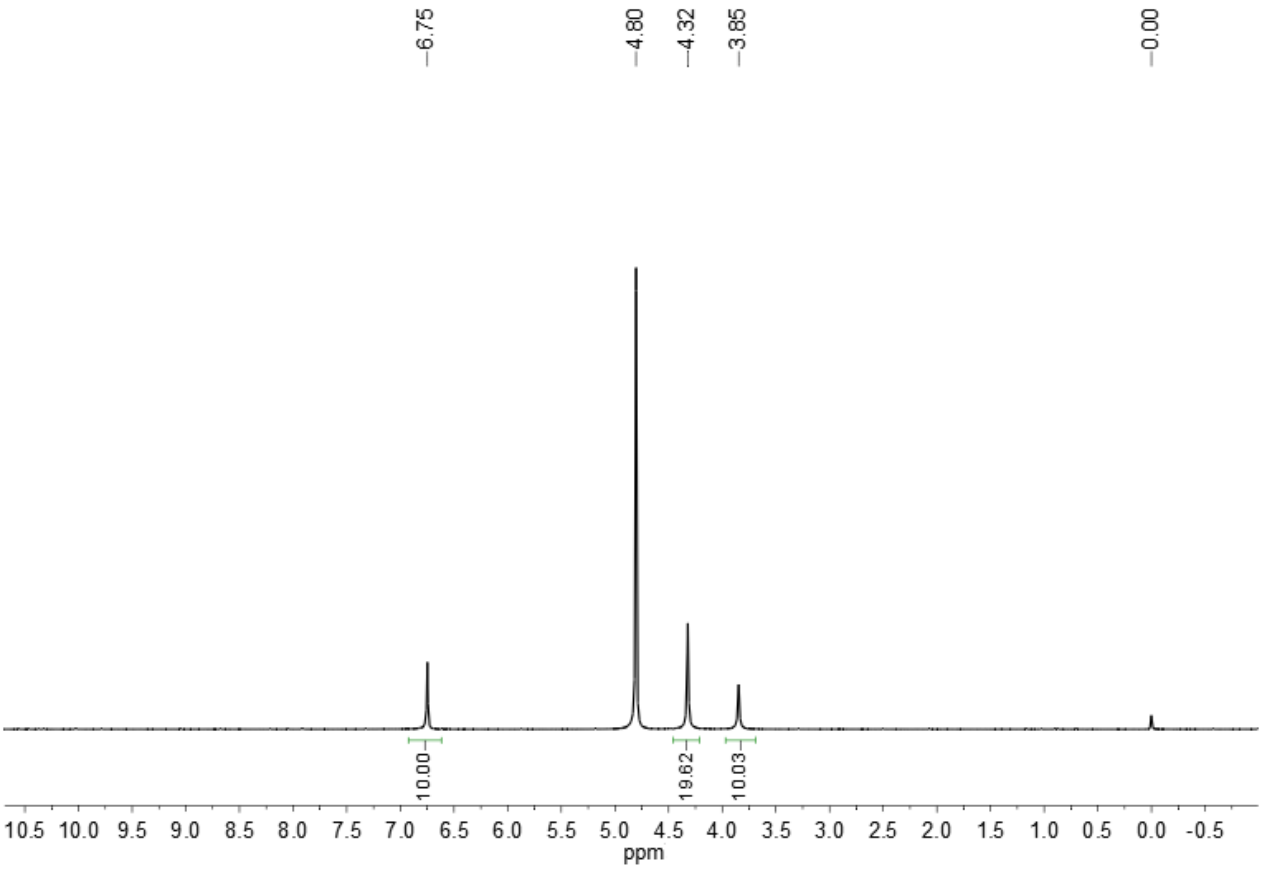

Fig. S2. ^{1}H NMR spectrum (400 MHz, D_2O, 20 °C) of **5**.

*3. Preparation of **3** and **4***

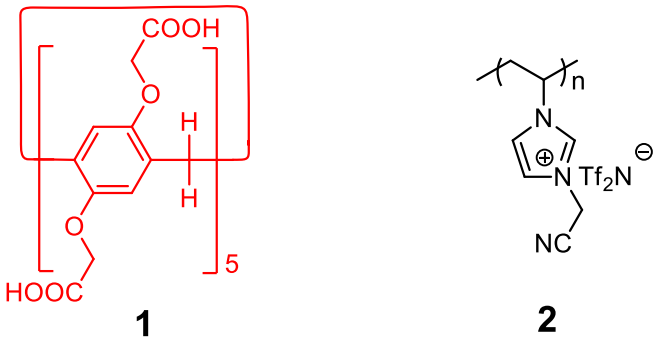

1 **2**

Scheme S2. Preparation of porous material **3** based on **1** and **2**.

PCMVImTf$_2$N (**2**) and fully carboxylic acid-substituted pillar[5]arene **1** were dissolved in DMSO at room temperature to form a solution, in which the PCMVImTf$_2$N concentration was kept at 10 wt%. The mole ratio of carboxylic acid groups on the pillar[5]arene to the repeating units on PCMVImTf$_2$N was fixed at 1.00. Then 3.00 mL of the solution was dropped (speed: 3.00 mL/min) into 30.0 mL of isopropanol containing 0.500 wt% of NH_3 (prepared by using 6 wt% aqueous NH_3 as ammonia source), which was placed in a glass beaker with stirring (900 rpm) and sonication (40% sonication amplitude). Sonication was applied for 1 min after the addition was finished. The precipitate was collected by centrifugation, washed by isopropanol three times, and dried under vacuum at 50 ^oC for 12 h. Elemental analysis: C, 50.70 ; H, 4.59 ; N, 14.47 ; S, 1.53.

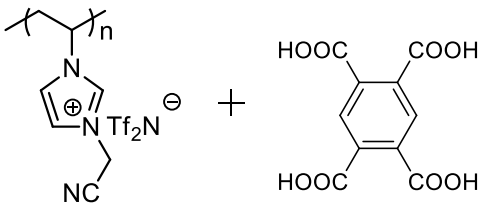

2

Scheme S3. Preparation of porous material **4** based on **2** and 1,2,4,5-benzenetetracarboxylic acid.

Porous material **4** was prepared according to our previous method.[S1] Nitrogen sorption measurements indicated that the specific Brunauer−Emmett−Teller (BET) surface area and the pore volume of **4** were calculated to be 310 m^2/g and 0.63 cm^3/g, respectively.[S1]

*4. FT-IR and XRD of **1** and **3***

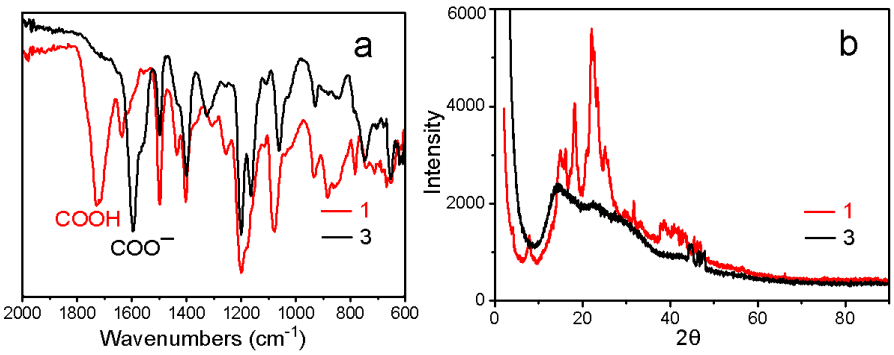

Fig. S3. (a) FT-IR of **1** and the pillar[5]arene cross-linked PIL network **3**; (b) XRD of **1** and **3**.

.

*5. SEM images of **3***

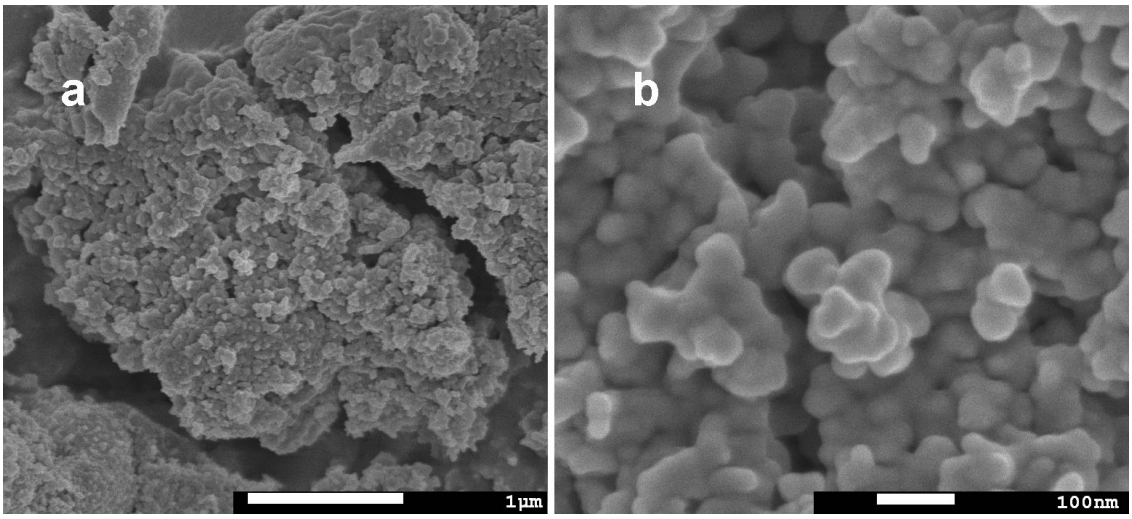

Fig. S4. SEM images of the porous material **3** at different scales.

*6. Pore size distribution curve of **3***

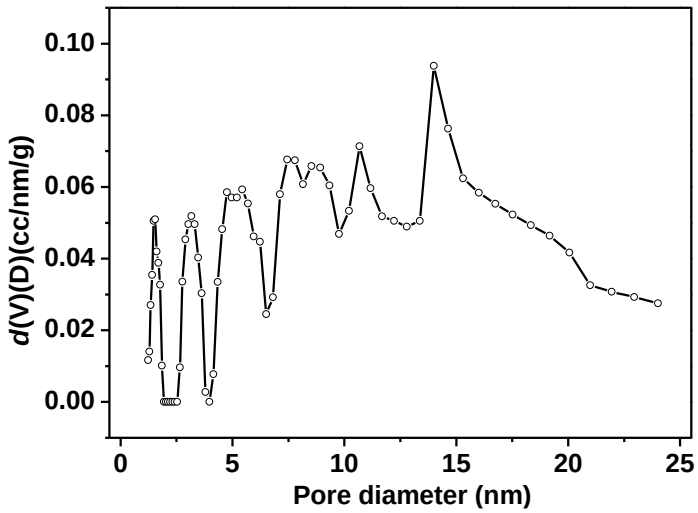

Fig. S5. Pore size distribution curve of pillar[5]arene-containing poly(ionic liquid) porous material **3**.

7. Complexation of 1,6-hexanediol and ***5***

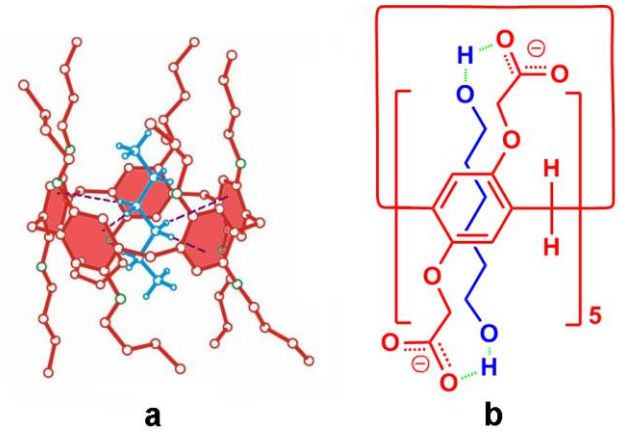

Fig. S6. a) Crystal structure of DBpillar[5]arene⊃*n*–hexane.[S3] b) Possible complexation mode of 1,6-hexanediol and **5**.

To investigate the host–guest binding properties of the pillar[5]arene in their superstructure, a suitable guest has to be selected. We had to choose neutral guests to avoid the strong electrostatic interactions between the porous network and charged guests weakening the selectivity of the pillar[5]arene recognition. To employ also the zwitterionic top and bottom groups of the current material, we selected a slightly more complicated separation problem, the binding of diols from their aqueous as well as organic solutions. This is a typical separation problem as it might turn up in green chemistry and biorefinery schemes.[S4]

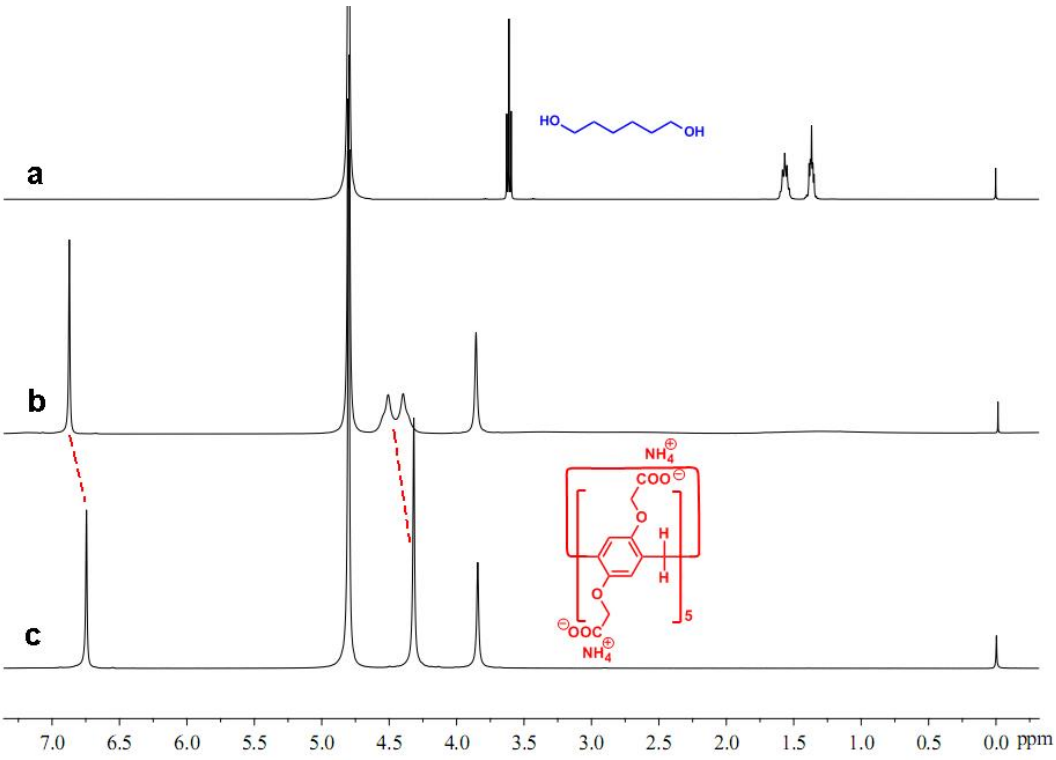

Fig. S7. Proton NMR spectra (400 MHz, D_2O. 25 ℃): a) 1,6-hexanediol; b) 8.00 mM 1,6-hexanediol and **5**; c) **5**. We could not measure their binding constants in chloroform, since neither the fully carboxylic acid-substituted pillar[5]arene **1** nor the fully carboxyl anion functionalized pillar[5]arene **5** is soluble in chloroform.

8. Proton NMR spectra of 1,6-hexanediol (in D_2O) after being treated with different materials

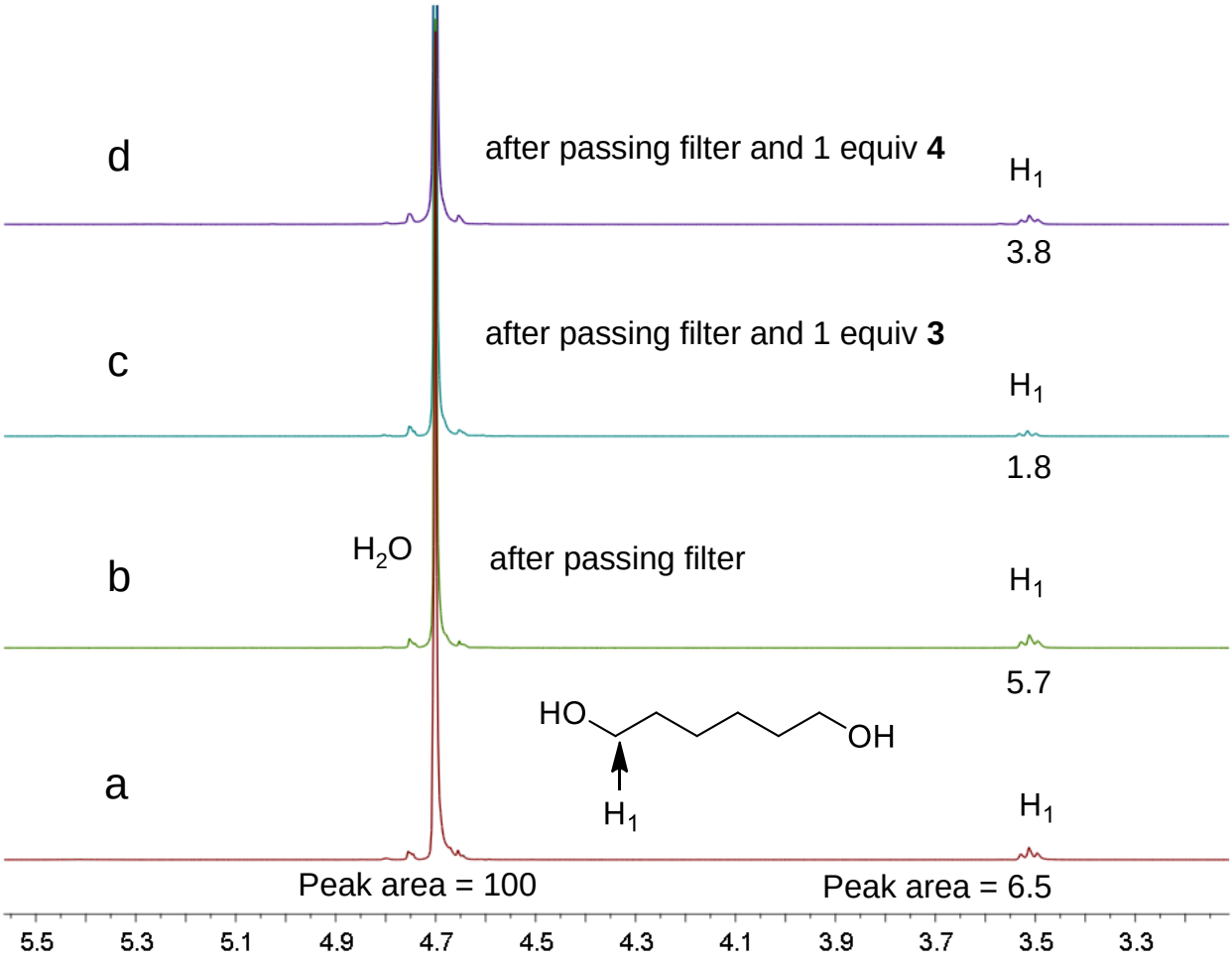

Fig. S8. Proton NMR spectra (400 MHz, 25 ℃) of 1.00 mM 1,6-hexanediol in D_2O: a) untreated; after being treated with b) filter, c) filter and 1 *equiv* pillar[5]arene-containing porous material **3**, and d) filter and 1 *equiv* pillar[5]arene-free porous material **4** for 1 h. H_2O was used as the reference, and the H_2O peak area was set as 100. It can be seen that the filter can absorb partial 1,6-hexanediol in aqueous solution due to the porous structure in the filter product. In addition, macro-/mesopores in pillar[5]arene-free porous material **4** (prepared from PCMVImTf_2N **2** and 1,2,4,5-benzenetetracarboxylic acid) can also absorb 1,6-hexanediol in aqueous solution. Finally compared to filter and **4**, the macro-/mesoporous pillar[5]arene-containing materials **3** absorbs the highest amount of 1,6-hexanediol due to the additional molecular recognition-induced adsorption.

*9. Proton NMR spectra of 1,6-hexanediol (in $CDCl_3$) after being treated with **3***

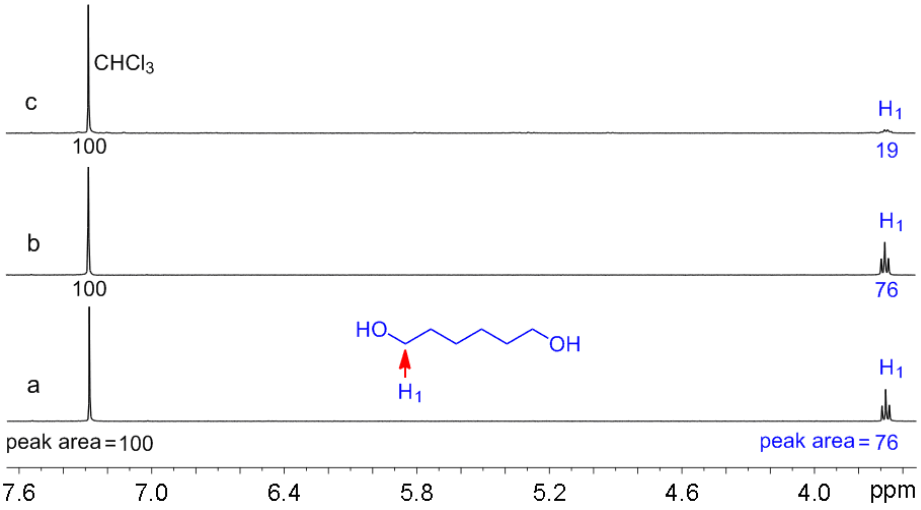

Fig. S9. (a) Proton NMR spectra (400 MHz, 25 ℃): 1.00 mM 1,6-hexanediol in $CDCl_3$; (b) through PTFE filter; (c) after being treated with 2.50 *equiv* porous material **3** for 1 h and PTFE filter. Here we used the residual $CHCl_3$ in $CDCl_3$ from one bottle as the reference, and set the $CHCl_3$ peak area at 100 to estimate the fraction of 1,6-hexanediol remaining in solution.

10. Proton NMR spectra of 1,6-hexanediol (in $CDCl_3$) after being treated with different materials

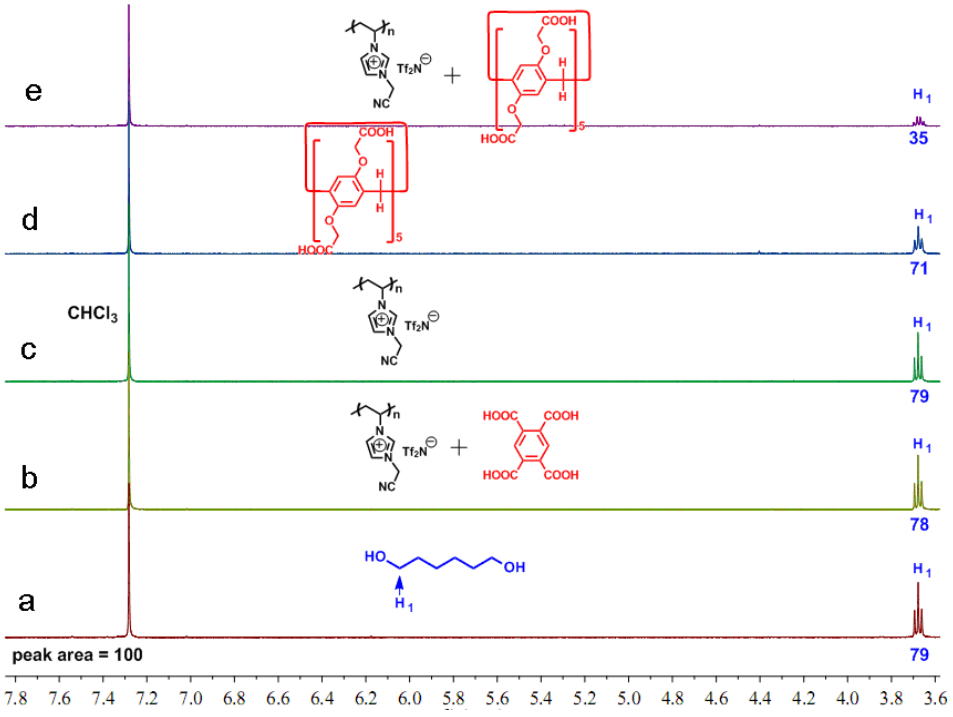

Fig. S10. Proton NMR spectra (400 MHz, 25 ℃) of 1.00 mM 1,6-hexanediol in $CDCl_3$: a) untreated; after being treated with b) 1 *equiv* **4**, c) 1 *equiv* **2**, d) 1 *equiv* **1**, and e) 1 *equiv* porous material **3** for 1 h. $CHCl_3$ was used as the reference, and the $CHCl_3$ peak area was set at 100. Compounds **1** (1.00×10^{-6} mol), **2** (containing 1.00×10^{-5} mol imidazolium), **3** (containing 1.00×10^{-6} mol **1** and 1.00×10^{-5} mol imidazolium), and **4** (containing 2.50×10^{-6} mol 1,2,4,5-benzenetetracarboxylic acid and 1.00×10^{-5} mol imidazolium) were used as adsorbents for 1.00 mL of a 1.00 mM $CDCl_3$ solution of 1,6-hexanediol separately.

*11. Percentages of 1,6-hexanediol in $CDCl_3$ after being treated with **3***

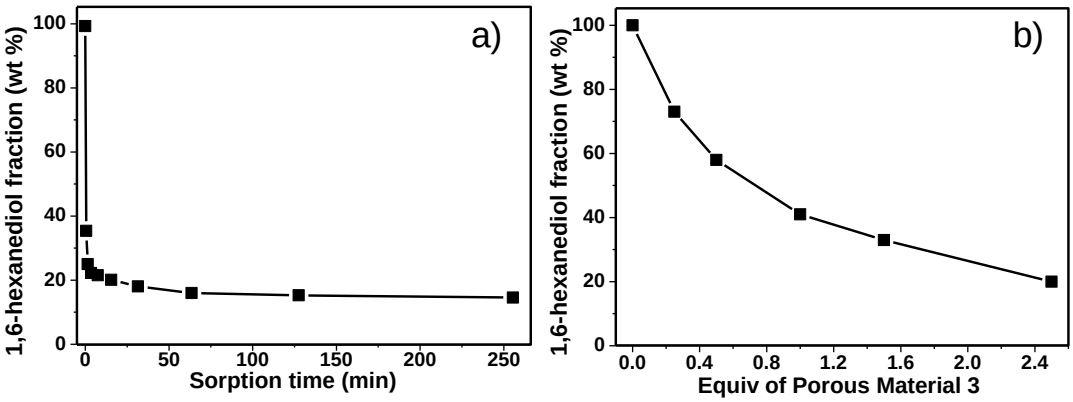

Fig. S11. Percentages of 1,6-hexanediol in $CDCl_3$ after being treated with: (a) 2 *equiv* **3** for different times; (b) different amounts of **3** for 1 h.

From Fig. S11, we found that the adsorption process is at first very fast: about 92% of the overall bound 1,6-hexanediol (80% with regard to the total amount) is adsorbed in the first minute, with the other 8% taking up to 1 h. These results indicated that the macro-/meso transport pore structure in **3** can effectively connect a majority of all inner pillar[5]arene pores with the outer environment in a rather efficient mass-transfer process. The second slower process is attributed to a much slow pore-to-pore hopping, which however is only active for a minority of the leftover inner pores. Fig. S11b showed the maximum adsorption capacities bound with different amounts of **3**. We found that the maximum amount of hexandiol bound increases with the increase of the amount of **3**, but the relative filling efficiency of the pillar[5]arene cavities decreased. This means that at the applied very low concentration of 1.00 mM, we are already in the limit of binding strength. The binding constant was calculated to be about 2900 M^{-1}. The binding constant (K_a) was calculated when **3** (containing equimolar **1**) was used as adsorbent for 1.00 mM $CDCl_3$ solution of 1,6-hexanediol and assuming all pillararene pores were accessible and uniformly dispersed. K_a = 0.56 mM / (0.44 mM × 0.44 mM) = 2900 M^{-1}. From the pores we can also learn that at least 80% of the supramolecular pores are indeed accessible, an unexpectedly high value, as one might also consider some of the pillararenes to be trapped deeply in the nanoparticles.

*12. SEM images of **2** and **4***

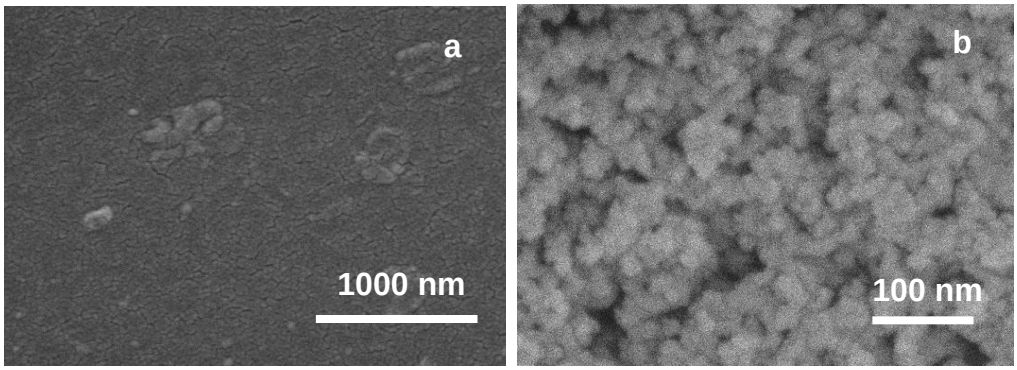

Fig. S12. SEM images of **2** (a) and **4** (b).

*13. XRD of **2** and **4***

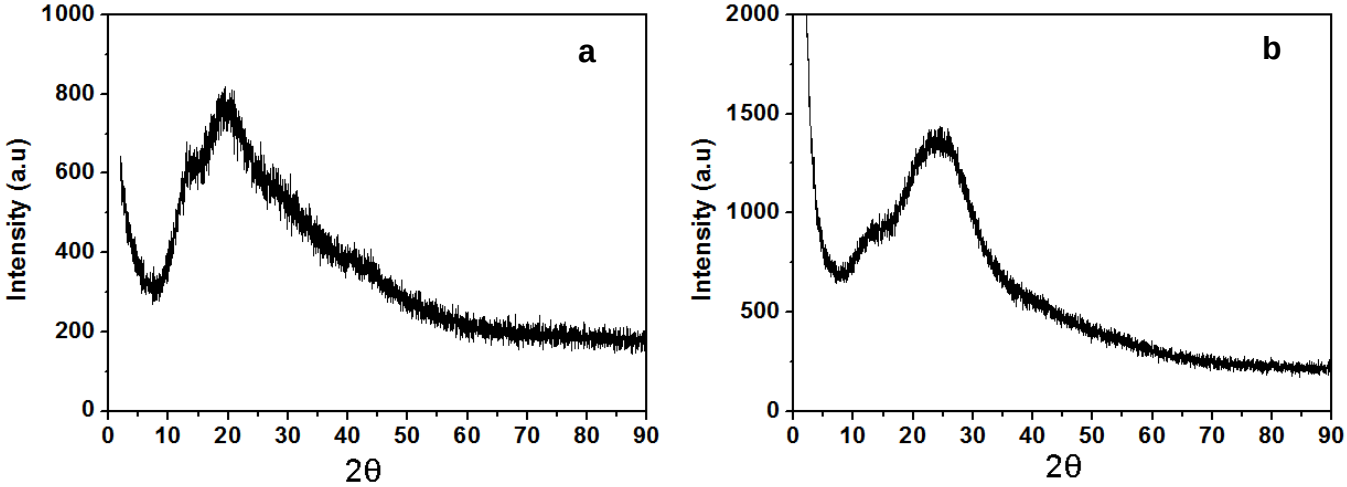

Fig. S13. (a) XRD of **2**; (b) XRD of **4**.

References:

S1 Q. Zhao, P. Zhang, M. Antonietti and J. Yuan, *J. Am. Chem. Soc.* **2012**, *134*, 11852–11855.

S2 T. Ogoshi, M. Hashizume, T.-a. Yamagishi and Y. Nakamoto, *Chem. Commun.* **2010**, *46*, 3708-3710.

S3 Z. Zhang, B. Xia, C. Han, Y. Yu and F. Huang, *Org. Lett.* **2010**, *12*, 3285-3287.

S4 (a) M. Blair, P. C.Andrews, B. H. Fraser, C. M. Forsyth, P. C. Junk, M. Massi and K. L. Tuck, *Synthesis* **2007**, 1523–1527; (b) C. D. Roy and H. C. Brown, *Tetrahedron Lett.* **2007**, *48*, 1959–1961.